LEVEL $\mathrm{I\!I}$ (12)

Nonlinear Theory and Experimental Observations of the Local Collisional Rayleigh-Taylor Instability in a Descending Equatorial Spread-F Ionosphere

M. J. KESKINEN AND S. L. OSSAKOW

Geophysical and Plasma Dynamics Branch
Plasma Physics Division

E. P. SZUSZCZEWICZ AND J. C. HOLMES

E.O. Hulburt Center for Space Research
Space Science Division

DTIC
SELECTED
FEB 0 9 1981
E

January 8, 1981

NAVAL RESEARCH LABORATORY
Washington, D.C.

81 2 09 002

NRL-MR-4311

REPORT DOCUMENTATION PAGE

1. REPORT NUMBER	2. GOVT ACCESSION NO.	3. RECIPIENT'S CATALOG NUMBER
NRL Memorandum Report 4399	AD-A094723	

4. TITLE *(and Subtitle)*	5. TYPE OF REPORT & PERIOD COVERED
NONLINEAR THEORY AND EXPERIMENTAL OBSERVATIONS OF THE LOCAL COLLISIONAL RAYLEIGH-TAYLOR INSTABILITY IN A DESCENDING EQUATORIAL SPREAD-F IONOSPHERE	Interim report on a continuing basis.
	6. PERFORMING ORG. REPORT NUMBER

7. AUTHOR(*s*)	8. CONTRACT OR GRANT NUMBER(*s*)
M. J. Keskinen, E. P. Szuszczewicz, S. L. Ossakow, and J. C. Holmes	S99QAXH I25AAXH

9. PERFORMING ORGANIZATION NAME AND ADDRESS	10. PROGRAM ELEMENT, PROJECT, TASK AREA & WORK UNIT NUMBERS
Naval Research Laboratory Washington, DC 20375	67-0889-0-0 71-0950-0-0

11. CONTROLLING OFFICE NAME AND ADDRESS	12. REPORT DATE
Defense Nuclear Agency Washington, DC 20305	January 1981
	13. NUMBER OF PAGES
	38

14. MONITORING AGENCY NAME & ADDRESS(*if different from Controlling Office*)	15. SECURITY CLASS. *(of this report)*
	UNCLASSIFIED
	15a. DECLASSIFICATION/DOWNGRADING SCHEDULE

16. DISTRIBUTION STATEMENT *(of this Report)*

Approved for public release; distribution unlimited.

17. DISTRIBUTION STATEMENT *(of the abstract entered in Block 20, if different from Report)*

18. SUPPLEMENTARY NOTES

This research was sponsored in part by the Defense Nuclear Agency under subtask S99QAXHC041, work unit 21, and work unit title "Plasma Structure Evolution;" and under subtask I25AAXHX640, work unit 12, and work unit title "Plasma Probe Data;" and the Office of Naval Research.

19. KEY WORDS *(Continue on reverse side if necessary and identify by block number)*

Nonlineary theory	Kwajalein 1979 campaign
Experimental observations	Collisional Rayleigh-Taylor instability
Computer simulations	Plasma probe data
Equatorial spread F	
Descending F layer	Wavelength

20. ABSTRACT *(Continue on reverse side if necessary and identify by block number)*

The nonlinear evolution of the local collisional Rayleigh-Taylor instability in downward-moving equatorial F layers has been studied in a coordinated theoretical and experimental program dealing with actual conditions of bottomside spread F. For ambient bottomside electron density gradient scale lengths L = 8 and 25 km, we find large percentage depletions and inverse power law spatial power spectra over the intermediate wavelength range λ = 25 m - 1 km. In addition we outline a nonlinear theory of the collisional Rayleigh-Taylor instability applicable to an upward or downward moving equatorial F region ionosphere. These results represent the first definitive comparison between experiment and theory with their agreement lending further support to the belief that the collisional Rayleigh-Taylor instability is responsible for large scale size irregularities that occur under conditions of equatorial spread F.

DD FORM 1473 EDITION OF 1 NOV 65 IS OBSOLETE
1 JAN 73
S/N 0102-LF-014-6601

CONTENTS

NONLINEAR THEORY AND EXPERIMENTAL OBSERVATIONS OF THE LOCAL COLLISIONAL RAYLEIGH-TAYLOR INSTABILITY IN A DESCENDING EQUATORIAL SPREAD-F IONOSPHERE

INTRODUCTION

Recently, coincident rocket and radar observations of equatorial spread-F were made near Kwajalein in the Marshall Islands [Szuszczewicz et al., 1980; Tsunoda, 1980a]. The in situ rocket data showed major plasma depletions distributed throughout a downward moving F-layer with regions of smaller scale in situ irregularities tending to be collocated with positive gradients of electron density. The VHF radar measurements showed that the backscatter "plumes", in addition to having large vertical extent from the bottomside to the topside [see also Kelley et al., 1976; McClure et al., 1977; Woodman and LaHoz, 1976], were identifiable with the plasma depletions [Tsunoda and Towle, 1979; Tsunoda, 1980b] and could be characterized by a growth and decay phase [Tsunoda, 1980a]. The recent rocket/radar comparison [Szuszczewicz et al., 1980] specifically showed that the most intense radar returns in the topside F-region were collocated with the upper region of a decay-phase depletion.

Several features of the small scale irregularity ($\lambda \leqslant 3m$) signatures seen by the radar backscatter can be explained by various plasma kinetic instabilities [for a review, see Ossakow, 1979] which are presumably driven by steep gradients within developing plasma bubbles. On the other hand, much evidence now exists that the large scale irregularities result from a Rayleigh-Taylor instability [Balsley et al., 1972; Haerendel, 1974] driven by the ambient bottomside plasma density gradient. Global [Scannapieco and Ossakow, 1976; Ossakow et al., 1979; Zalesak and Ossakow, 1980] and local [Keskinen et al., 1980] numerical simulations of the collisional Rayleigh-Taylor instability have successfully reproduced the large plasma density depletions (bubbles) and associated spatial power spectra that have been experimentally observed.

The most recent in situ rocket observations [Szuszczewicz et al., 1980] were made in an F-layer that was moving downward, implying the existence of a large scale westward electric field. The importance of this electric field in describing the development of plasma bubbles has been discussed by several authors [Ossakow and Chaturvedi, 1978; Ossakow et al., 1979; Ott, 1978; Anderson and Haerendel, 1979]. However, all previous analytical and numerical studies of the nonlinear collisional Rayleigh-Taylor instability have not included the effects of an upward or downward moving F-layer in realistic geometries, nor have they had the opportunity for an almost ideal comparison with experimental results.

In this paper we study the nonlinear evolution of the collisional Rayleigh-Taylor instability in a vertically convecting F layer using both analytical and numerical techniques. In addition we compare the simulations with the recent in situ rocket data which provided direct measurements of gradient scale lengths and density fluctuation power spectra.

EXPERIMENTAL RESULTS

By 2100 (LT) on 17 July 1979 the bottomside of the F-region at Kwajalein had risen to an approximate altitude of 400 km. The F-layer then began a downward drift with an approximate velocity $V_D \simeq 10$ m/sec [Szuszcezewicz et al., 1980; R. Tsunoda, private communication, 1980] and a simultaneous onset of spread-F. With the F-layer drifting downward and spread-F conditions continuing, a rocket (designated PLUMEX I) was launched (00:31:30, July 17, 1979 LT) when the bottomside F-layer had descended to an altitude below 300 km.

2

A pair of pulsed probes [Szuszczewicz and Holmes, 1977; and associated references] were diametrically extended from the forward end of the rocket payload. The sensing elements, constructed from tungsten wire, were isolated from their extension booms by coaxial guard electrodes driven at the same potential as the probes themselves. One of the probes, defined as the I-probe, operated with a baseline voltage $V_B \approx -1v$, yielding net ion baseline current I_B^i. The other probe, defined as the E-probe, operated with $V_B \approx +2v$, yielding net electron baseline current I_b^e. Both probes generated complete current-voltage characteristics in $\tau_s \approx 400$ msec, yielding absolute values of N_e and T_e at an approximate 2.5 Hz rate. Maximum I_B sampling occurred at 2048 Hz, resulting in 0.5 meter spatial resolution for relative electron density fluctuations at a vehicle velocity of 1 km/sec. (See Szuszczewicz and Holmes, 1980 for instrument details and complete payload configuration.)

Figure 1 displays the upleg measurements of relative and absolute electron density as extracted from the pulsed-plasma-probe data. Absolute values of electron density were determined by conventional analyses of Langmuir probe characteristics [Chen, 1965] with appropriate care to eliminate perturbing effects of surface contamination [Szuszczewicz and Holmes, 1975], density fluctuations [Holmes and Szuszczewicz, 1975; Szuszczewicz and Holmes, 1977] and magnetic field effects [Szuszczewicz and Takacs, 1979]. Analysis of approximately 25 characteristics were executed over the F-layer from 340-560 km. In each case a conversion coefficient $a \equiv N_e \, [cm^{-3}]/I_e(V^+)$ was determined so that the $I_e(V^+)$ profile in Figure 1 could be directly scaled to absolute electron densities. This procedure yielded $a = (5.5 \pm 0.5) \, 10^{10}$ electrons $cm^{-3}A^{-1}$. The results in Figure 1 show the F-peak at 375 km with a maximum density of $1.3 \, (10^6) \, cm^{-3} \, (\pm 10\%)$. The probe measurements also revealed a number of major depletions ($\delta N_e/N_e^o \lesssim 90\%$) distributed throughout

3

the F-region. Each of the depletions has been shown to have its own set of smaller scale irregularities [Szuszczewicz et al., 1980; Szuszczewicz and Holmes, 1980] with the most intense percent fluctuations occurring on the bottomside gradient near 270 km (Region "C" in Szuszczewicz et al., 1980).

The pulsed probe data provided an excellent opportunity for comparison with the numerical simulations of the collisonal Rayleigh-Taylor (R-T) instability at intermediate wavelengths (e.g., Keskinen et al., 1980). Attention is focused on the depleted structure on the bottomside F-layer gradient near 270 km which is believed representative of the mid-phase development of the R-T process. (We will follow Szuszczewicz et al., 1980 and refer to this domain as region "C".) An expanded view of this domain (Fig. 2) shows that it is not a single macroscale depletion but a region of contiguous large scale structures extending over a total altitude domain of about 12 km. (Vehicle velocity in region "C" was 2.4 km/sec.)

Typically, computer simulations employ several values for the zero-order gradient scale length

$$ L = \left(\frac{1}{N_e^o} \frac{dN_e^o}{dy} \right)^{-1} $$

and initialize the simulation with a two-dimensional perturbation. In the work of Keskinen et al. [1980] L was selected to be 5, 10 and 15 km and the perturbation took the form([Chaturvedi and Ossakow, 1977]).

$$ \frac{\delta N_e(x,y,t=0)}{N_e^o} = (10^{-4}) \; \text{Sin} \; (k_y \; y) \; \text{Cos} \; (k_x \; x) + 2(10^{-6}) \; \text{Sin} \; (2k_y \; y) $$

with k_x and k_y being the horizontal and vertical wavenumbers, respectively. Both k_x and k_y were set equal to $2\pi/960$ m in the simulation. In addition, the computation assumed that L was centered at 300 km. Under actual conditions encountered in PLUMEX I, the bottomside F-layer gradient extended from 240 to 290 km.

The question of gradient scale length can be studied in Figure 3 where it is shown that the bottomside gradient (encompassed in the 105-125 sec time frame) is not characterized by a single value of L. Experimentally, L was computed according to $<I_B> (dI_B/dy)^{-1}$ with $<I_B>$ and the altitude derivative determined from sliding linear fits to the I_B data set. In region "C" (114s $\leqslant$ t $\leqslant$ 122s) L is seen to vary between 2 and 10 km, whereas adjacent domains (110s $\leq$ t $\leq$ 113s and 122s $\leq$ t $\leq$ 126s) can be characterized by L = 25 km.

Previous computer simulations [Keskinen et al., 1980], conducted with L = 5, 10 and 15 km, gave evidence that linearly unstable modes saturate by nonlinear generation of linearly damped vertical modes. The results yielded one-dimensional power laws (horizontal and vertical) that vary with a spectral index ($\equiv$ n in $P_{N_e} \propto k^{-n}$) between 2.0 and 2.5. To explore this result within the context of region "C", and to provide important comparisons with simulations in the next sections , power spectral analyses were conducted over sliding intervals of 2.4 km. The results, presented in Figure 4, show that the dominant behavior is $k^{-2.5}$ over the range k = $2\pi/1$km to k $\approx 2\pi/25$ m. The $k^{-1.85}$ behavior at t = 116.001 sec is a result of the very sharp density gradient (see region "C" Fig. 2) encompassed by the domain of the spectral analysis. (We note that the spectral analysis is executed on a time (frequency)-domain function I_B and the conversion to k-space is made under the assumption $\wedge = vf^{-1}$, where v is the vehicle velocity.)

5

In general we would conclude that our observed large depletions and spatial power spectra support the numerical simulations of <u>Keskinen et al.</u> (1980). Further testing of this support is achieved in the next sections which present simulations with L = 8 and 25 km with a downward drifting F-layer model that is more in keeping with the actual experimental conditions. The F-layer time-history can be important since unstable modes require times in excess of 4,000 seconds to saturate...a time during which the F-layer encountered in PLUMEX I drifted downward in excess of 40 km.

MODEL EQUATIONS

The two fluid equations describing the Rayleigh-Taylor instability in the presence of a zeroth-order horizontal westward electric field $\underline{E}_0$ can be written, after invoking quasineutrality ($n_e \approx n_i \approx n$),

$$\frac{\partial n_\alpha}{\partial t} + \nabla \cdot (n_\alpha \underline{V}_\alpha) = -\nu_R (n_\alpha - n_{\alpha 0}) \tag{1}$$

$$0 = -T_e \nabla n_e - e n_e \left(-\nabla \varphi + \frac{\underline{V}_e \times \underline{B}_0}{c} + \underline{E}_0 \right) \tag{2}$$

$$m_i n_i \left(\frac{\partial}{\partial t} + \underline{V}_i \cdot \nabla \right) \underline{V}_i = -T_i \nabla n_i + e n_i \left(-\nabla \varphi + \frac{\underline{V}_i \times \underline{B}_0}{c} + \underline{E}_0 \right)$$

$$\tag{3}$$

$$+ m_i n_i \underline{g} - m_i n_i \nu_{in} \underline{V}_i$$

$$\nabla \cdot \underline{J} = 0 \tag{4}$$

$$\underline{J} = n_e (\underline{V}_i - \underline{V}_e) \tag{5}$$

where α denotes electrons (e) or ions (i) and n, φ, $\underline{V}$, ν_R, ν_{in}, $\underline{B}_0$, and $\underline{g}$

6

are the density, electrostatic potential, velocity, recombination coefficient, ion-neutral collision frequency, magnetic field, and gravity respectively. In addition, we have written the total electric field $\underline{E} = -\nabla\varphi + \underline{E}_o$. All other symbols retain their conventional meaning. Since we will be interested in studying intermediate wavelengths ($\lambda \sim 100m - 1$ km) we ignore inertial and pressure effects in (1) - (5). Setting $\nabla\varphi = \nabla\varphi_1 + m_i\underline{g}/e$ [Ossakow et al., 1979], solving algebraically (2) and (3) for the velocities $\underline{V}_e$, $\underline{V}_i$, using (4) and the ion continuity equation (1), we find

$$\frac{\partial n}{\partial t} - \frac{c}{B}(\nabla_\perp\varphi_1 \times \hat{z}) \cdot \nabla_\perp n = -\nu_R(n - n_o) \tag{6}$$

$$\nabla_\perp \cdot (\nu_{in} n \nabla_\perp\varphi_1) = \frac{B}{c}(\underline{g}\times\hat{z}) \cdot \nabla_\perp n + \underline{E}_o \cdot \nabla_\perp(\nu_{in}n) \tag{7}$$

We have written eq. (6) and (7) in a downward moving frame whose velocity is $\underline{V}_D = c\,\underline{E}_o \times \underline{B}/B^2 \simeq 10$ m/sec and have adopted the following coordinate system: the magnetic field $\underline{B}$ is in the z-direction (north), the y-direction (vertical) denotes altitude with $\underline{g} = -g\hat{y}$ and the x-axis points westward. By linearizing (6) and (7) and writing $\delta n \equiv n - n_o$, $\varphi_1 \propto \exp\lceil i(k_x x + k_y y) + \gamma_{\underline{k}} t]$, $\underline{k} \cdot \underline{B} = 0$, and $|\underline{k}|L \gg 1$ we find

$$\gamma_{\underline{k}} = \left(\frac{g}{\nu_{in}} \pm \frac{cE_o}{B}\right)\left(\frac{k_x}{k}\right)^2\frac{1}{L} - \nu_R \tag{8}$$

where $\underline{E}_o = \mp E_o\hat{x}$, $L = \left(\frac{1}{n_o}\frac{\partial n_o}{\partial y}\right)^{-1}$, $k^2 = k_x^2 + k_y^2$.

From (8) we note that we recover the usual collisional Rayleigh-Taylor instability if $E_o \rightarrow 0$. The growth rate $\gamma_{\underline{k}}$ is enhanced (reduced) by an

7

eastward (westward) electric field E_o. We will be concerned only with a westward electric field ($\underline{E}_c = \underline{E}_o \hat{x}$) which leads to a downward moving F layer.

NUMERICAL SIMULATIONS

Be defining $n'(x,y) = n(x,y)/n_o(y)$, $\varphi_1'(x,y) = \varphi_1(x,y)/BL$, $x' = x/L$, $y' = y/L$, $t' = ct/L$ where $n_o(y) = N_o(1 + y/L)$ ($N_o = $ const.) is an equilibrium solution of (6) and (7) we can write (6) and (7) in dimension-less form as follows (after dropping primes for clarity):

$$\frac{\partial n}{\partial t} - \frac{\partial \varphi_1}{\partial y}\frac{\partial n}{\partial x} + \frac{\partial \varphi_1}{\partial x}\frac{\partial n}{\partial y} = \frac{n}{n_o}\frac{\partial n_o}{\partial y}\frac{\partial \varphi_1}{\partial x} - \beta_1(n - 1) \qquad (9)$$

$$\frac{\partial^2 \varphi_1}{\partial x^2} + \frac{\partial^2 \varphi_1}{\partial y^2} + \left(\frac{1}{n}\frac{\partial n}{\partial y} + \frac{1}{n_o}\frac{\partial n_o}{\partial y}\right)\frac{\partial \varphi_1}{\partial y} + \frac{1}{n}\frac{\partial n}{\partial x}\frac{\partial \varphi_1}{\partial x} = -\beta_2\frac{1}{n}\frac{\partial n}{\partial x} \qquad (10)$$

where $\beta_1 = L\nu_R/c$ and $\beta_2 = g/c\nu_{in} - E_o/B$ are dimensionless constants. Equation (9) was integrated forward in time using a flux-corrected [Boris and Book, 1973] leapfrog-trapezoidal scheme [Zalesak, 1979] while eq. (10) was solved for the self-consistent potential φ_1 using a Chebychev semi-iterative multigrid technique [McDonald, 1980]. The computational grid described a small vertical slice oriented in the east-west direction of the bottomside equatorial F layer and is defined by 64 x 64 points with a constant mesh spacing of $\Delta x = \Delta y = 15$m giving an altitude and east-west extent of 960 meters. Periodic boundary conditions were imposed on n/n_o and φ_1 in both the x (east-west) and y (vertical) directions.

The in situ rocket data of Szuszczewicz and Holmes [1980] do not reveal the initial conditions from which the observed irregularities developed.

8

Many sets of initial conditions are possible. In the context of the experimental observations of an initially upward and then downward moving F layer [Tsunoda, 1980a; Szuszczewicz et al., 1980], we make the reasonable assumption that the irregularities, whose spatial power spectra are sampled in Region "C" [Szuszczewicz and Holmes, 1980] of the bottomside, originate at a higher altitude(s) y_0 at earlier time(s) and are convected downward by the ambient F layer. This is in agreement with the conclusions of Narcisi and Szuszczewicz (1980) in their analysis of ion composition measurements conducted on the same rocket. From previous numerical simulations [Keskinen et al., 1980] of the intermediate wavelength collisional Rayleigh-Taylor instability for bottomside gradient scale lengths L = 5 - 15 km at an altitude of 300 km, we found that a well-developed nonlinear regime could be achieved after a time $\Delta t \simeq 10\text{-}15\ \gamma_m^{-1}$ where γ_m is the maximum linear growth rate. We define the altitude of instability onset y_0 to be the position of the bottomside gradient at $\Delta t \simeq 10\text{-}15\ \gamma^{-1}$ sec prior to the time of rocket penetration. (The rocket penetrated region "C" on the bottomside at an altitude of 270 km.) This, of course, neglects the fact that $\gamma(y)$ will be decreasing since ν_{in} and ν_R will be increasing [see eq. (8)] for a downward moving F layer. In other words we wish to determine an altitude $y_0 - 15\gamma^{-1}(y)v_D = 270$ km where $v_D = 10$ m/sec. For L = 8 km (25 km) we find $y_0 \simeq 335$ km (365 km). From the Jacchia [1965] model neutral atmosphere [Ossakow et al., 1979], ν_{in} (335 km) $\simeq 0.3$ sec^{-1}, ν_{in} (365 km) $\simeq 0.18$ sec^{-1}, ν_R (335 km) $\simeq 1 \times 10^{-4}$ sec^{-1}, ν_R (365 km) $\simeq 4.5 \times 10^{-5}$ sec^{-1} and $\Omega_i = 300$ sec^{-1}. Coupling these considerations with the probe measurements of gradient scale lengths, two different numerical simulations were made using L = 8 and 25 km. Both simulations were initialized with the following density profile: $n(x,y,t = 0)/N_0 = 1 + y/L + \epsilon(x,y)$ where $\epsilon(x,y)$ is a random function

of position in the xy-plane with a white noise-like spatial power spectrum (no preferred wavelength) and a root-mean-square amplitude of 0.03.

Since the real space dimensions of the computational grid are 960 m by 960 m, the altitude dependent quantities $\nu_{in}(y)$ and $\nu_R(y)$ do not, at any fixed time, vary appreciably over the grid since their scale heights are much greater than the grid dimensions. In fact, these quantities can be fit very well with exponential variation in y, i.e., $\nu_{in}(y) \propto \exp(-y/L_{in})$ and $\nu_R(y) \propto \exp(-y/L_R)$ with $L_{in} \simeq 55$ km and $L_R \simeq 33$ km between the altitudes of 250 and 550 km using a <u>Jacchia</u> [1965] model neutral atmosphere [<u>Ossakow et al.</u>, 1979]. However, over several thousands of seconds, ν_{in} and ν_R will change (increase) in a frame moving downward with velocity $v_D = 10$ m/sec. In order to compensate for this effect, we convert the spatial (altitude) dependence of ν_{in} and ν_R into functions of time by making the substitution $y \rightarrow - v_D t$. In other words, during the course of the simulations, $\nu_{in}(t) = \nu_{in}(t_o) \exp(v_D\Delta t/L_{in})$ and $\nu_R(t) = \nu_R(t_o) \exp(v_D\Delta t/L_R)$ where Δt is elapsed time and $\nu_{in}(t_o)$, $\nu_R(t_o)$ are the initial values depending upon initial altitude. In this simple model we ignore any variation of the bottomside density gradient scale length with altitude. We now present the important nonlinear aspects of these simulations.

Figure 5 gives an isodensity contour plot of $\widetilde{\delta n}(x,y) \equiv \delta n/n_o(y)$, $\delta n = n(x,y) - n_o(y)$, at $t = 800$ sec for $L = 8$ km and shows that the random nature of the initial perturbations still prevails. The contours of the random initial perturbations in $\widetilde{\delta n}(x,y)$ at $t = 0$ sec are very similar to Figure 5 but with more smaller scale structure. Figure 6 displays the evolution of $\widetilde{\delta n}(x,y)$ at $t = 2000$ sec where some vertical elongation and steepening can be seen together with small scale irregularities. Figure 7 illustrates the

perturbation density contours at t = 4500 sec where further steepening and vertical elongation have occurred. This late time density configuration is similar to recent numerical simulations of the intermediate wavelength collisional Rayleigh-Taylor instability [Keskinen et al., 1980] under almost monochromatic initial conditions, i.e., with only two waves initially excited. The maximum percentage depletion ($\widetilde{\delta}n < o$) in Fig. 7 was 56%. Similar density contour development and late time percentage depletion were found using L = 25 km and again starting from random initial conditions. These large depletions were also noted in the in situ rocket data of Szuszczewicz and Holmes [1980].

In Figures 8a and 8b we have plotted sample one-dimensional horizontal $P(k_x)$ and vertical $P(k_y)$ spatial power spectra for $2\pi/k_x$, $2\pi/k_y$ between approximately 100m and 960m in the nonlinear regime for L = 8 km at t = 4000 sec. These power spectra are obtained by integrating $|\widetilde{\delta}n(k_x,k_y)|^2$ over k_y and k_x, respectively. The spectral indices obtained from these power spectra are in agreement with those derived from bottomside irregularity power spectra as determined from rocket observations [Region "C" of Szuszczewicz and Holmes, 1980] in the wavelength domain λ: 25m - 1km (see Fig. 4) and recent simulations [Keskinen et al., 1980]. Similar power laws and spectral indices were found for the L = 25 km case but on a longer time scale.

NONLINEAR THEORY

We wish to interpret the evolution of long wavelength plasma irregularities in an upward or downward moving equatorial F region ionosphere in terms of coherent two-dimensional mode-coupling among collisional Rayleigh-Taylor modes. This type of analysis was also used to study large scale wavelengths excited by the gradient drift instability in the equatorial electrojet [Rognlien and Weinstock, 1974] and the saturation of the long wavelength local collisional [Chaturvedi and Ossakow, 1977] and collisionless

11

[Hudson, 1978] Rayleigh-Taylor instability in equatorial spread F. However, these latter papers did not include the effects of a convecting (rising or falling) background ionosphere which usually accompanies equatorial spread F. The linear growth rate $\gamma_{\underline{k}}$ (eq. 8) which contains the altitude dependent parameters ν_R and ν_{in}, and, by inference, the nonlinear growth rate will change in space and time in a vertically convecting ionosphere. Since with vertical drift velocities of the order of 10 m/sec the F region ionosphere can convect over a distance on the order of the scale height of υ_{in} and υ_R on time scales comparable to the nonlinear saturation times of the collisional Rayleigh-Taylor instability, this effect will be important.

We begin our nonlinear analysis with eq. (6) and (7) which can be written

$$\frac{\partial \delta n}{\partial t} - \frac{c}{B} \nabla_{\perp} \phi_1 \times \underline{\hat{z}} \cdot \nabla n_o + \nu_R \delta n = \frac{c}{B} \nabla_{\perp} \phi_1 \times \underline{\hat{z}} \cdot \nabla \delta n \qquad (11)$$

$$(c/B\Omega_i) \nabla_{\perp} \cdot \nu_{in} n \nabla \phi_1 = (\underline{g} \times \underline{\hat{z}}/\Omega_i + c\nu_{in}\underline{E}_o/B) \cdot \nabla \delta n \qquad (12)$$

where we have made the separation $\delta n = n - n_o$. We note that the addition of a large scale electric field $\underline{E}_o$ in (12) adds only a linear term. The convective nonlinear term on the righthand side of (11) is the dominant nonlinearity since the ratio of the nonlinear terms in (11) and (12) is

$$(c/B\Omega_i)(\nabla_{\perp} \cdot \nu_{in} n \nabla \phi_1)/(c/B)\nabla_{\perp}\phi_1 \times \underline{\hat{z}} \cdot \nabla \delta n \sim \nu_{in}/\Omega_i \ll 1$$

12

for two dimensional perturbations ϕ_1 and δn. This allows one to find the potential perturbation ϕ_1 for arbitrary density perturbation δn using a linearized version of (12), i.e.,

$$\frac{e\varphi_1}{T} = -i\beta \frac{\delta n}{n_o} \tag{13}$$

where, keeping the same notation as Chaturvedi and Ossakow [1977] , $\beta = (g/\nu_{in})(k_x \Omega_i/k^2 c_s^2)$ with $c_s^2 = T/m_i$. Equation (11) can then be rewritten

$$\frac{\partial \delta n}{\partial t} = \gamma_{\underline{k}} \, \delta n + \frac{c}{B} \, \nabla \phi_1 \times \hat{\underline{z}} \cdot \nabla \delta n \tag{14}$$

with $\gamma_{\underline{k}}$ given by (8). If we take an arbitrary two-dimensional perturbation of the form

$$\frac{\delta n}{n_o} = A_{1,1} \sin (k_x x - \omega t) \cos k_y y \tag{15}$$

where the first subscript on A denotes the vertical mode number and the second subscript signifies the horizontal mode number, we find using (13) the associated potential perturbation

$$\frac{e\varphi_1}{T} = \beta A_{1,1} \cos (k_x x - \omega t) \cos k_y y \tag{16}$$

Then the nonlinear self-interaction $\frac{c}{B} \nabla \phi_1 \times \hat{\underline{z}} \cdot \nabla \delta n$ generates a term of the form $n_o \, \alpha/2 \, A_{1,1}^2 \sin 2k_y y \equiv A_{2,0} \sin 2k_y y$ with $\alpha \equiv k_x^2 k_y g/k^2 \nu_{in}$ which is linearly damped by recombination using (14). This linearly damped mode

$A_{2,0}$ will interact through the nonlinearity in (14) with $A_{1,1}$ to give a nonlinear damping for the linearly unstable mode $A_{1,1}$ since

$$\frac{c}{B} \nabla\varphi_{1,1} \times \hat{z} \cdot \nabla\delta n_{2,0} = -2\alpha n_o A_{1,1} A_{2,0} \sin (k_x x - \omega t) \cos k_y y$$

$$\cos 2k_y y.$$

In other words, a two dimensional linearly unstable perturbation with amplitude $A_{1,1}$ can generate a linearly damped vertical mode $A_{2,0}$ which, in turn, can react back to stabilize the $A_{1,1}$ mode.

In the frame of reference of a small localized region in the bottomside of a downward convecting F layer we assume $\nu_{in} = \nu_{in}(t)$ and $\nu_R = \nu_R(t)$ are monotonically smooth functions of time as in the previous simulations. Then for a general perturbation of the form

$$\frac{\delta n}{n_o} = A_{1,1} \sin (k_x x - \omega t) \cos k_y y + A_{2,0} \sin 2k_y y \qquad (17)$$

we can write

$$\frac{\partial A_{1,1}}{\partial t} = \gamma_{1,1}(t) A_{1,1} - 2 \alpha(t) A_{1,1} A_{2,0} \qquad (18)$$

$$\frac{\partial A_{2,0}}{\partial t} = - |\gamma_{2,0}(t)| A_{2,0} + \frac{\alpha(t)}{2} A_{1,1}^2 \qquad (19)$$

where now the growth rate $\gamma(t)$ and nonlinear coupling coefficient $\alpha(t)$ are functions of time since they contain altitude dependent quantities

ν_{in} and ν_R. In deriving (18) and (19) we have assumed that $\gamma(t)$ and $\alpha(t)$ are weakly time dependent. For $\underline{E}_o \to 0$ (stationary F region), we recover the results of Chaturvedi and Ossakow [1977] who treated γ and α as space and time independent. Since $\alpha \sim 1/\nu_{in}$, one observes that the nonlinear coupling decreases (increases) for a downward (upward) drifting F layer since ν_{in} increases (decreases). Assuming that a quasi-steady state is achieved at $t = t_s$ with $\partial A_{1,1}/\partial t \simeq \partial A_{2,0}/\partial t \simeq 0$, we obtain from (18) and (19)

$$A_{2,0}(t_s) = \gamma_{1,1}(t_s)/2\alpha(t_s) \simeq 1/2 \; k_y L \tag{20}$$

$$A_{1,1}(t_s) = (2 \; |\gamma_{2,0}(t_s)| A_{2,0}/\alpha(t_s))^{\frac{1}{2}}$$

$$\simeq ((k^2/k_x^2)(\nu_R(t_s)\nu_{in}(t_s)/gLk_y^2))^{\frac{1}{2}} \tag{21}$$

Since $A_{2,0}(t_s)$ is independent of ν_{in} and ν_R we note from (20) and (21) that the two dimensional spatial power spectra of the density fluctuations in a rising or falling F region ionosphere will have the oblique linearly un- stable modes, e.g., $A_{1,1}$ being favored at low altitudes (increasing ν_R and ν_{in}) with the linearly damped waves, e.g., $A_{2,0}$ dominating at higher altitudes (decreasing ν_R and ν_{in}) with spatial power spectra $\propto k_y^{-2}$. Indeed for $k_y \simeq k_x$ we can write

$$A_{2,0}(t_s)/A_{1,1}(t_s) \simeq (1/2\sqrt{2}) \; (g/\nu_{in}(t_s)\nu_R(t_s)L)^{\frac{1}{2}}$$

so that at 300 km with L = 25 using a <u>Jacchia</u> [1965] model neutral atmosphere [<u>Ossakow et al.</u>, 1979] we find $A_{2,0} \sim A_{1,1} \sim 1\%$ for $k_x L = 2\pi L/\lambda_x \simeq 50$ while at 425 km $A_{2,0}/A_{1,1} \sim 10$. A more detailed examination of the static and dynamic solutions of (18) and (19) will be reserved for a future report.

SUMMARY

We have performed analytical and numerical simulations studies of the collisional Rayleigh-Taylor instability in local unstable regions of downward-moving equatorial F layers. For ambient bottomside plasma density gradient scale lengths $L = 8$ and 25 km, we have demonstrated that large percentage relative depletions can develop on time scales of several thousands of seconds from purely random initial conditions. In addition we have shown that the one-dimensional spatial power spectra of these irregularities in the vertical and east-west directions conform to power laws $\propto k^{-n}$, $n = 2-2.5$ for $2\pi/k$ between 100m and 1 km. These results are in good agreement with our recent in situ rocket observations of intermediate wavelength (λ: 25m - 1 km) irregularities equatorial spread-F, presented here in this paper, complement previous local numerical simulations [Keskinen et al., 1980] , and lend further support to the belief that the collisional Rayleigh-Taylor instability is responsible for large scale size irregularities in equatorial spread-F.

Future work will include global simulations of upward and downward moving equatorial F layers together with the inclusion of neutral wind effects.

17

ACKNOWLEDGMENTS

REFERENCES

Anderson, D. N., and G. Haerendel, The motion of depleted plasma regions in the equatorial ionosphere, J. Geophys. Res., 84, 4251, 1979.

Balsley, B. B., G. Haerendel and R. A. Greenwald, Equatorial spread F: Recent observations and a new interpretation, J. Geophys. Res., 77, 5625, 1972.

Boris, J. P., and D. L. Book, Flux-corrected transport, I, Shasta, a transport algorithm that works, J. Comput. Phys., 11, 38, 1973

Chaturvedi, P.K., and S. L. Ossakow, Nonlinear theory of the collisional Rayleigh-Taylor instability in equatorial spread F, Geophys. Res. Lett., 4, 558, 1977.

Chen, F. F., Electrical probes, in Plasma Diagnostic Techniques, edited by R. H. Huddlestone and S. L. Leonard, Academic, New York, 1965, p. 113.

Haerendel, G. Theory of equatorial spread F, report, Max-Planck Inst. fur Phys. und Astrophys., Garching, West Germany, 1974.

Holmes, J. C. and E. P. Szuszczewicz, A versatile plasma probe, Rev. Sci. Instr. 46, 592, 1975.

Hudson, M. K., Spread F bubbles: Nonlinear Rayleigh-Taylor mode in two dimensions, J. Geophys. Res., 83, 3189, 1978.

Jacchia, L. G., Static diffusion models of the upper atmosphere with empirical temperature profiles, Smithson, Contrib. Astrophys., 8, 215, 1965.

Kelley, M. C., G. Haerendel, H. Kappler, A. Valenzuela, B. B. Balsley, D. A. Carter, W. L. Ecklund, C. W. Carlson, B. Hausler, and R. Torbert, Evidence for a Rayleigh-Taylor type instability and upwelling of depleted density regions during equatorial spread F, Geophys. Res. Lett., 3, 448, 1976.

Keskinen, M. J., S. L. Ossakow, and P. K. Chaturvedi, Preliminary report of numerical simulations of intermediate wavelength collisional Rayleigh-Taylor instability in equatorial spread F, J. Geophys. Res., 85, 1775, 1980.

McClure, J. P., W. B. Hanson, and J. H. Hoffman, Plasma bubbles and irregularities in the equatorial ionosphere, J. Geophys. Res., 82, 2650, 1977.

McDonald, B. E., Explicit Chebychev-iterative solution of nonself-adjoint elliptic equations on a vector computer, J. Comput. Phys., (in press), 1980.

Narcisi, R. S., and E. P. Szuszczewicz, Direct measurements of electron density, temperature and ion composition in an equatorial spread F ionosphere, Sixth International Symposium on Equatorial Aeronomy (Aguadilla, P. R., July, 1980); J. Atm. Terr. Phys. (to be published, 1980).

Ossakow, S. L., and P. K. Chaturvedi, Morphological studies of rising equatorial spread F bubbles, J. Geophys. Res., 83, 2085, 1978.

Ossakow, S. L., S. T. Zalesak, B. E. McDonald, and P. K. Chaturvedi, Nonlinear equatorial spread F: Dependence on altitude of F peak and bottomside background electron density gradient scale length, J. Geophys. Res., 84, 17, 1979.

Ossakow, S. L., Ionospheric irregularities, Rev. Geophys. and Space Phys., 17, 521, 1979.

Ott, E., Theory of Rayleigh-Taylor bubbles in the equatorial ionosphere, J. Geophys. Res., 83, 2055, 1978.

Rognlien, T. D. and J. Weinstock, Theory of the nonlinear spectrum of the gradient drift instability in the equatorial electrojet, J. Geophys. Res., 79, 4733, 1974.

Scannapieco, A. J. and S. L. Ossakow, Nonlinear equatorial spread F, Geophys. Res. Lett., 3, 451, 1976.

Szuszczewicz, E. P., R. T. Tsunoda, R. Narcisi and J. C. Holmes, Coincident radar and rocket observations of equatorial spread F, Geophys. Res. Lett., 7, 537, 1980.

Szuszczewicz, E. P. and J. C. Holmes, Equatorial spread F: "in situ" measurements of electron density, temperature, and density fluctuation power spectra, NRL Memo Report #4289, August 25, 1980.

Szuszczewicz, E. P., and J. C. Holmes, Observations of electron temperature gradients in mid-latitude E_s layers, J. Geophys. Res., 82, 5073, 1977.

Szuszczewicz, E. P., and J. C. Holmes, Surface contamination of active electrodes in plasmas: Distortion of conventional Langmuir probe measurements, J. Appl. Phys., 46, 5134, 1975.

Szuszczewicz, E. P. and P. Z. Takacs, Magnetosheath effects on cylindrical Langmuir probes, Phys. Fluids, 22, 2424, 1979.

Tsunoda, R. T., and D. M. Towle, On the spatial relationship of 1-meter equatorial spread-F irregularities and depletions in total electron content, Geophys. Res. Letts., 6, 873, 1979.

Tsunoda, R. T., Time evolution and dynamics of equatorial backscatter plumes-1. Growth phase, submitted to J. Geophys. Res., 1980a.

Tsunoda, R. T., On the spatial relationship of 1-meter equatorial spread-F irregularities and plasma bubbles, J. Geophys. Res., 85, 185, 1980b.

Woodman, R. F., and C. LaHoz, Radar observations of F-region equatorial irregularities, J. Geophys. Res., 81, 5447, 1976.

Zalesak, S. T., Fully multi-dimensional flux-corrected transport, J. Comput. Phys., 31, 355, 1979.

Zalesak, S. T., and S. L. Ossakow, Nonlinear equatorial spread F: spatially

large bubbles resulting from large horizontal scale initial perturbations,

J. Geophys. Res., 85, 2131, 1980.
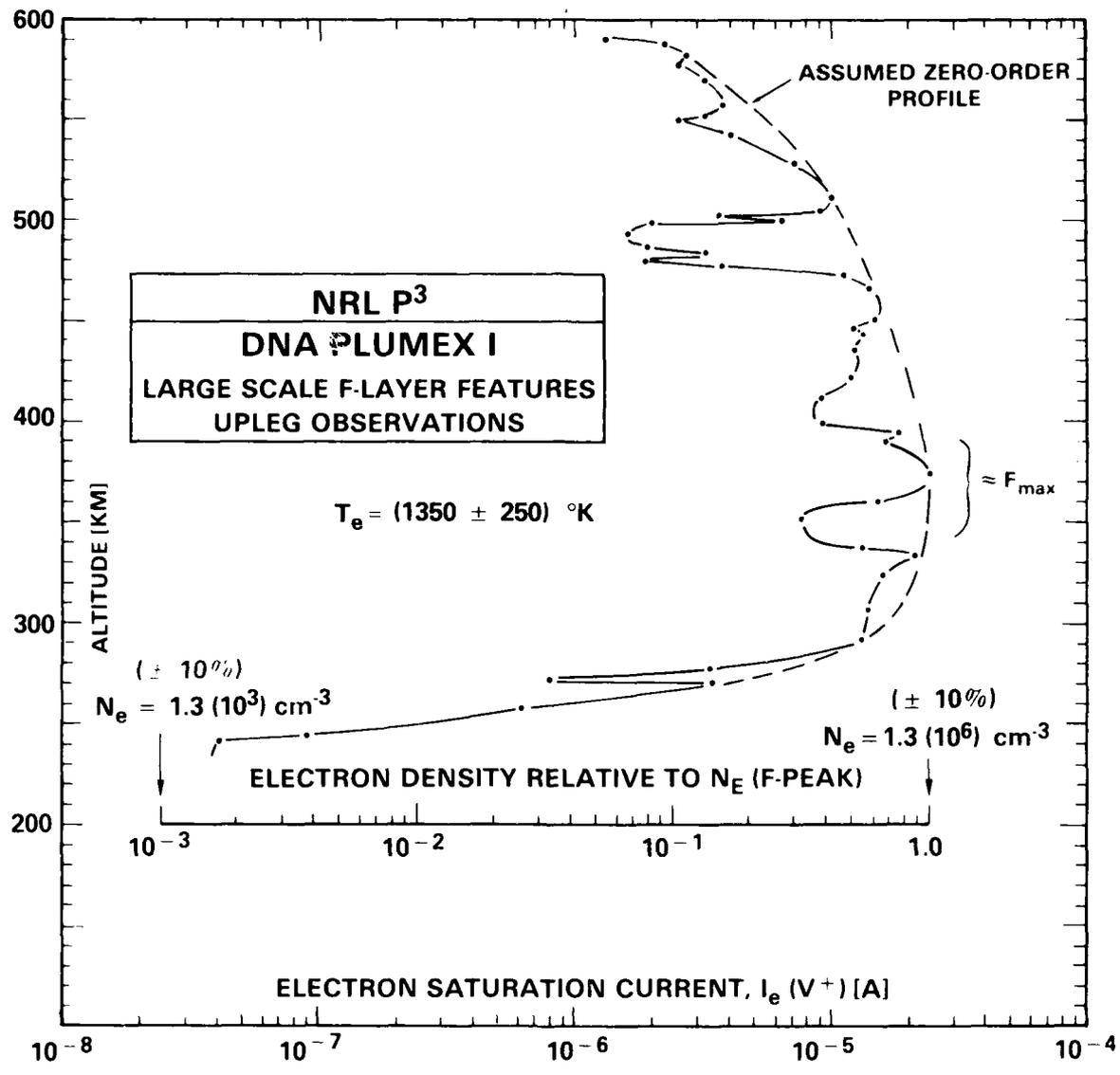
Fig. 1 — Relative and absolute ionospheric electron density profile determined in situ during the occurrence of equatorial spread F.
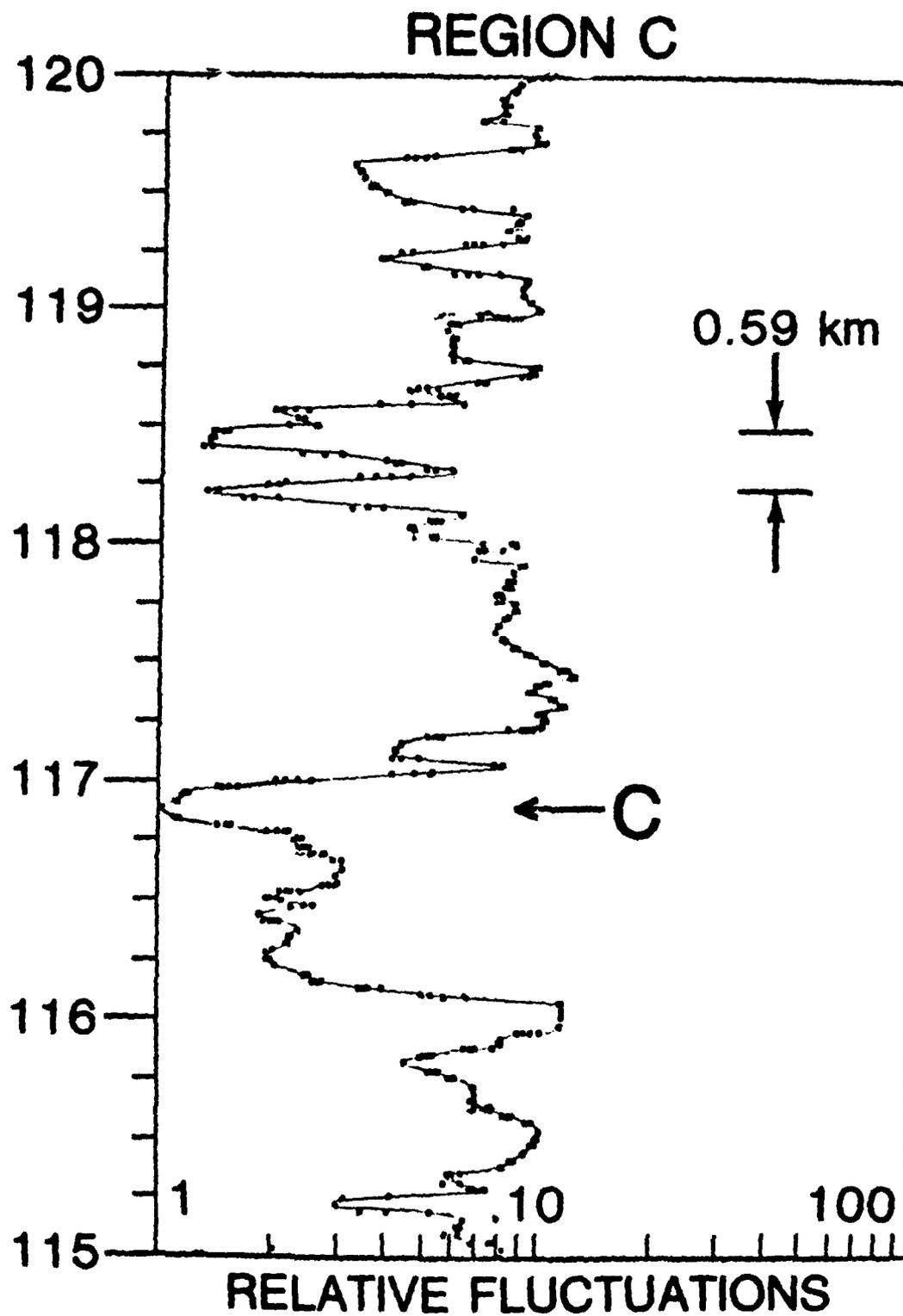
Fig. 2 — Expanded view of density fluctuation observed in the bottomside irregularity (Fig. 1) centered near 270 km. This is region "C" of Szuszczewicz et al. [1980].
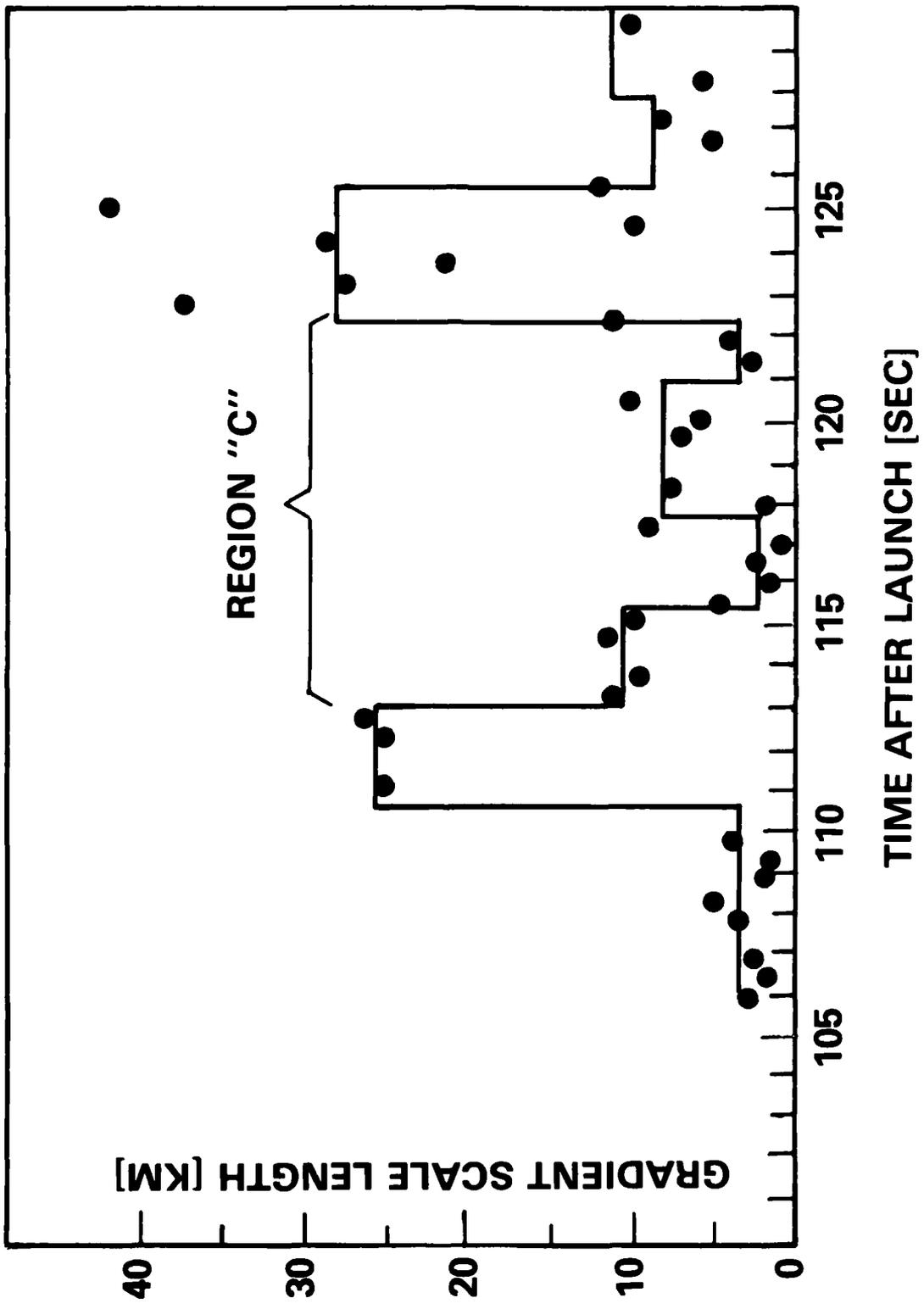
Fig. 3 — Gradient scale lengths on the bottomside ledge of the F-region layer shown in Figure 1.
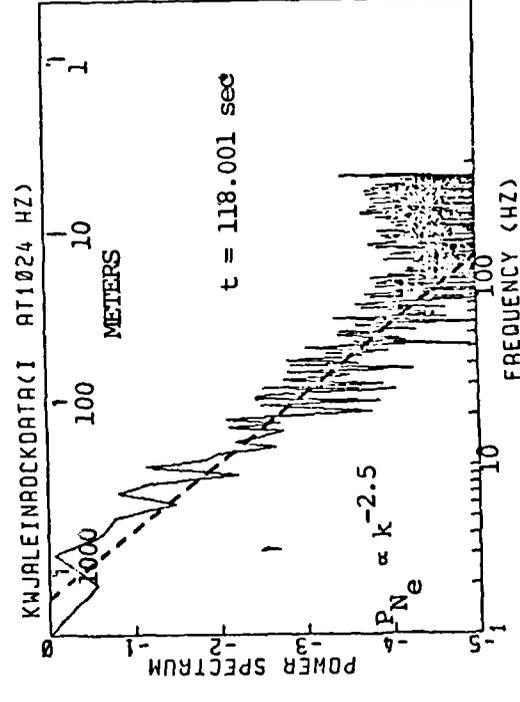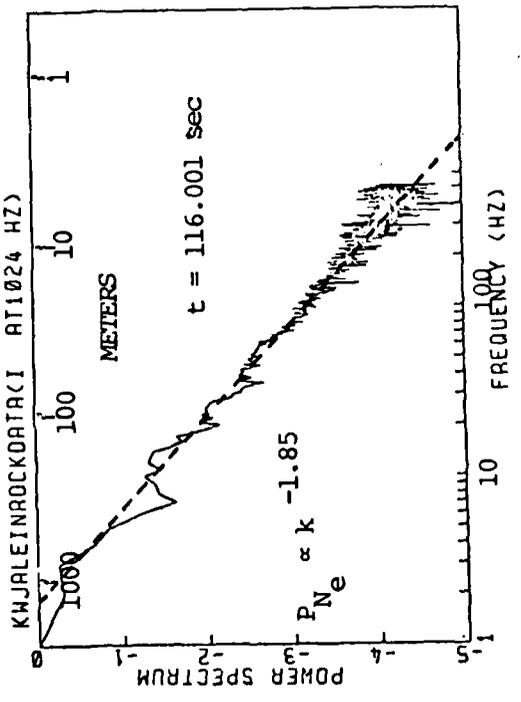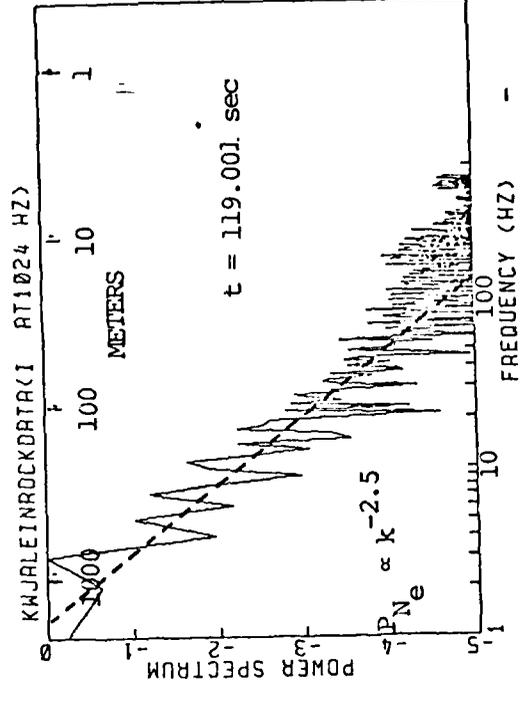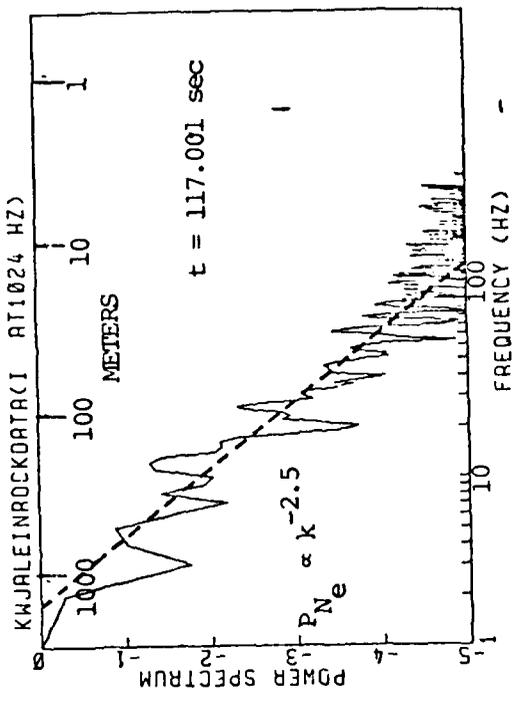
Fig. 4 — Power spectral analyses of density fluctuations in region "C" (Figure 2).
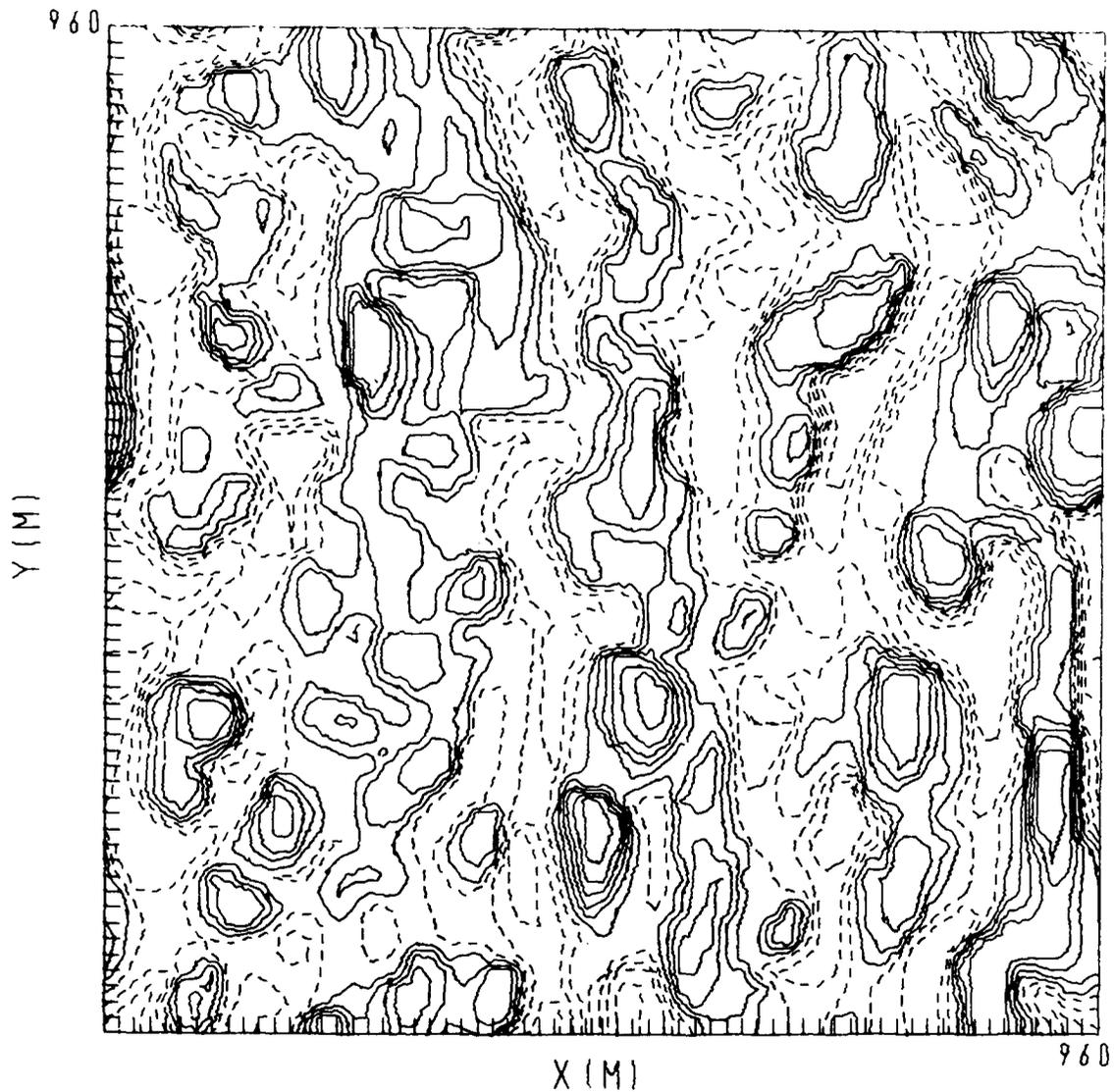
Fig. 5 — Isodensity contours of $\delta n(x,y)/n_o(y)$ for L = 8 km at t = 800 sec. Solid contours denote $\delta n/n_o > 0$; dashed contours denote $\delta n/n_o > 0$. Contours are evenly spaced with y axis vertical and x axis horizontal. Tick marks and numbers denote grid point locations and size of grid in meters, respectively. Maximum enhancement ($\delta n/n_o > 0$) and depletion ($\delta n/n_o > 0$) are + 4.8% and - 3.8%.
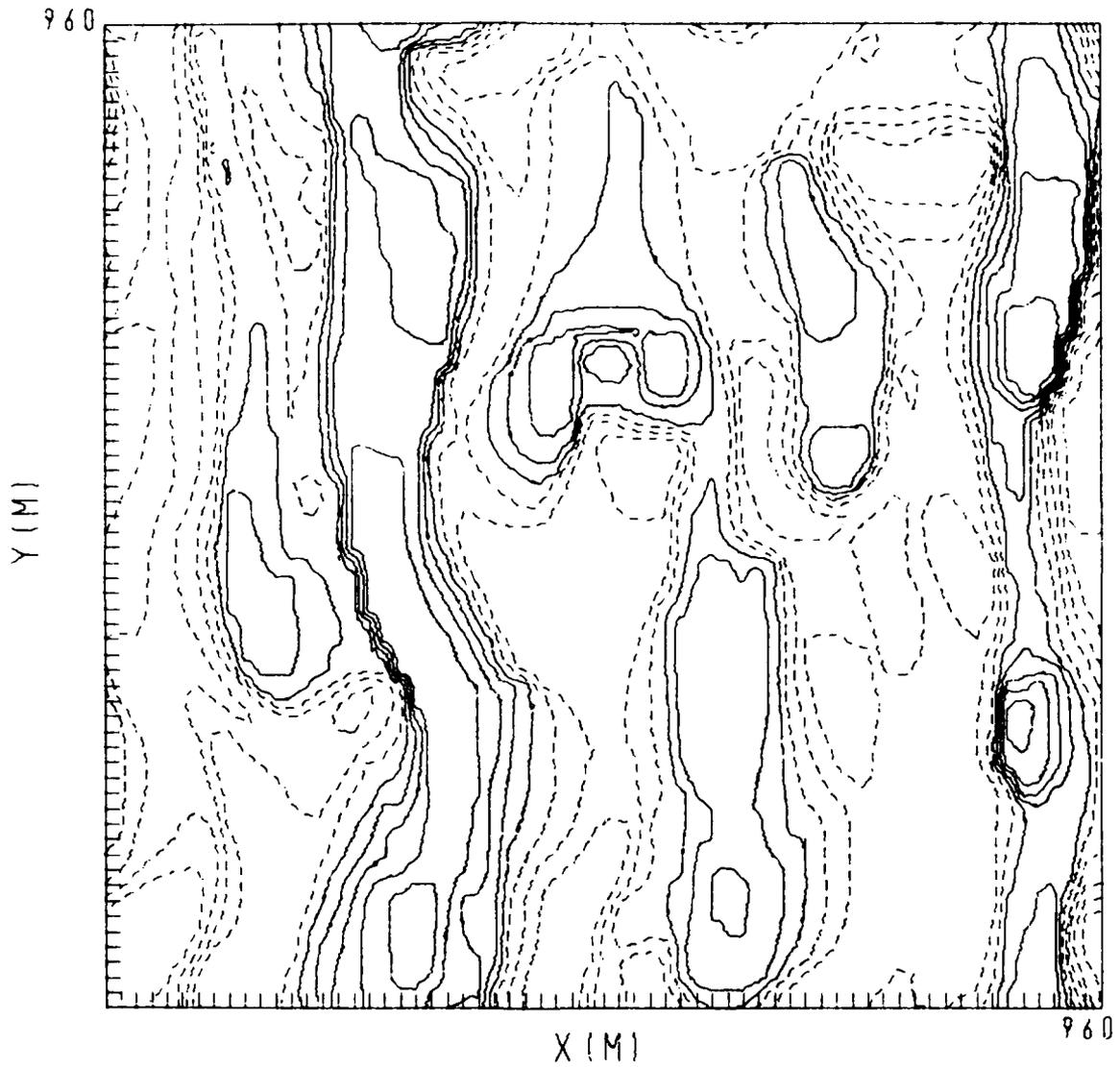
Fig. 6 — Same as Figure 5 but at t = 2000 sec. Maximum enhancement
and depletion are + 15% and - 11%.
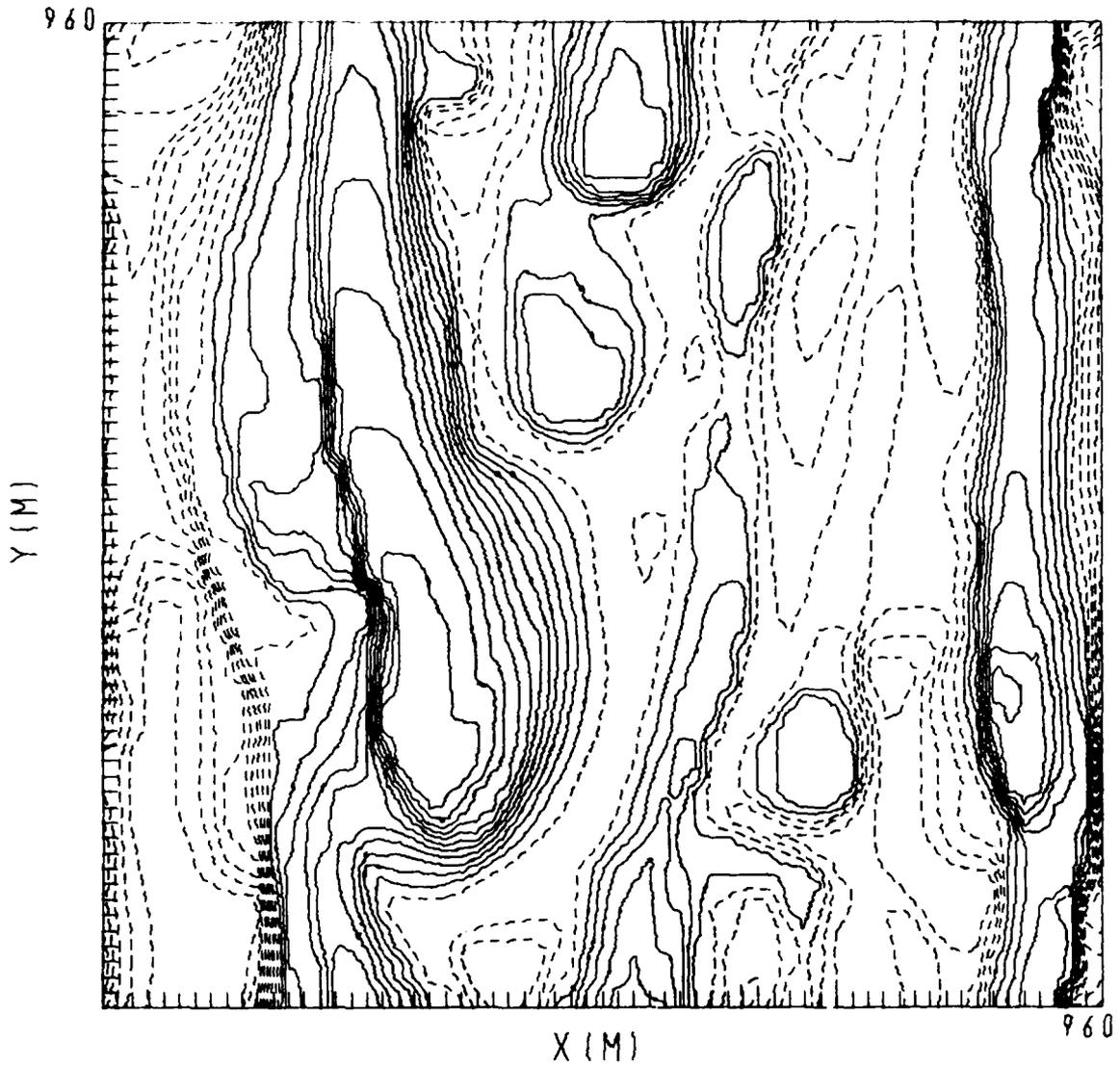
Fig. 7 — Same as Figure 5 but at t = 4500 sec. Maximum enhancement and
depletion are + 66% and - 56%.
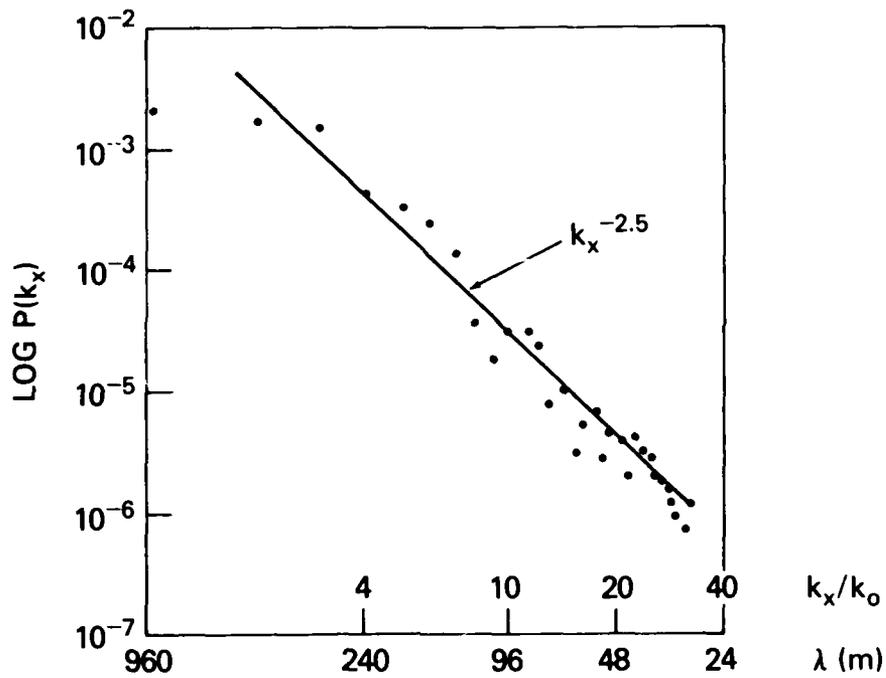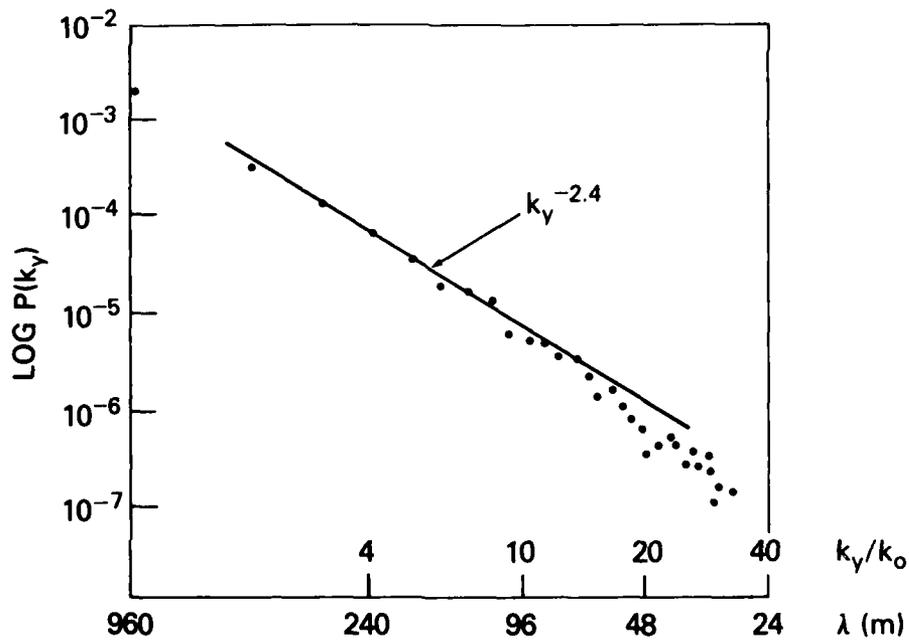
Fig. 8 — One-dimensional (a) horizontal $P(k_x)$ and (b) vertical $P(k_y)$ spatial power spectra versus k_x and k_y, respectively, for $L = 8$ km at $t = 4000$sec. The solid lines are least squares fits to the numerical simulations (dots) and $k_o = 2\pi/960$m.

30

DISTRIBUTION LIST

DEPARTMENT OF DEFENSE

ASSISTANT SECRETARY OF DEFENSE
COMM, CMD, CONT & INTELL
WASHINGTON, D.C. 20301
    01CY ATTN J. BABCOCK
    01CY ATTN M. EPSTEIN

ASSISTANT TO THE SECRETARY OF DEFENSE
ATOMIC ENERGY
WASHINGTON, D.C. 20301
    01CY ATTN EXECUTIVE ASSISTANT

DIRECTOR
COMMAND CONTROL TECHNICAL CENTER
PENTAGON RM BE 685
WASHINGTON, D.C. 20301
    01CY ATTN C-650
    01CY ATTN C-312 R. MASON

DIRECTOR
DEFENSE ADVANCED RSCH PROJ AGENCY
ARCHITECT BUILDING
1400 WILSON BLVD.
ARLINGTON, VA. 22209
    01CY ATTN NUCLEAR MONITORING RESEARCH
    01CY ATTN STRATEGIC TECH OFFICE

DEFENSE COMMUNICATION ENGINEER CENTER
1860 WIEHLE AVENUE
RESTON, VA. 22090
    01CY ATTN CODE R820
    01CY ATTN CODE R410 JAMES W. MCLEAN
    01CY ATTN CODE R720 J. WORTHINGTON

DIRECTOR
DEFENSE COMMUNICATIONS AGENCY
WASHINGTON, D.C. 20305
      (ADR CNWDI: ATTN CODE 240 FOR)
    01CY ATTN CODE 101B

DEFENSE TECHNICAL INFORMATION CENTER
CAMERON STATION
ALEXANDRIA, VA. 22314
    (12 COPIES IF OPEN PUBLICATION, OTHERWISE 2 COPIES)
    12CY ATTN TC

DIRECTOR
DEFENSE INTELLIGENCE AGENCY
WASHINGTON, D.C. 20301
    01CY ATTN DT-1B
    01CY ATTN DB-4C E. O'FARRELL
    01CY ATTN DIAAP A. WISE
    01CY ATTN DIAST-5
    01CY ATTN DT-1BZ R. MORTON
    01CY ATTN HQ-TR J. STEWART
    01CY ATTN W. WITTIG DC-7D

DIRECTOR
DEFENSE NUCLEAR AGENCY
WASHINGTON, D.C. 20305
    01CY ATTN STVL
    04CY ATTN TITL
    01CY ATTN DDST
    03CY ATTN RAAE

COMMANDER
FIELD COMMAND
DEFENSE NUCLEAR AGENCY
KIRTLAND AFB, NM 87115
    01CY ATTN FCPR

DIRECTOR
INTERSERVICE NUCLEAR WEAPONS SCHOOL
KIRTLAND AFB, NM 87115
    01CY ATTN DOCUMENT CONTROL

JOINT CHIEFS OF STAFF
WASHINGTON, D.C. 20301
    01CY ATTN J-3 WWMCCS EVALUATION OFFICE

DIRECTOR
JOINT STRAT TGT PLANNING STAFF
OFFUTT AFB
OMAHA, NB 68113
    01CY ATTN JLTW-2
    01CY ATTN JPST G. GOETZ

CHIEF
LIVERMORE DIVISION FLD COMMAND DNA
DEPARTMENT OF DEFENSE
LAWRENCE LIVERMORE LABORATORY
P. O. BOX 808
LIVERMORE, CA 94550
    01CY ATTN FCPRL

DIRECTOR
NATIONAL SECURITY AGENCY
DEPARTMENT OF DEFENSE
FT. GEORGE G. MEADE, MD 20755
    01CY ATTN JOHN SKILLMAN R52
    01CY ATTN FRANK LEONARD
    01CY ATTN W14 PAT CLARK
    01CY ATTN OLIVER H. BARTLETT W32
    01CY ATTN R5

COMMANDANT
NATO SCHOOL (SHAPE)
APO NEW YORK 09172
    01CY ATTN U.S. DOCUMENTS OFFICER

UNDER SECY OF DEF FOR RSCH & ENGRG
DEPARTMENT OF DEFENSE
WASHINGTON, D.C. 20301
    01CY ATTN STRATEGIC & SPACE SYSTEMS (OS)

WWMCCS SYSTEM ENGINEERING ORG
WASHINGTON, D.C. 20305
    01CY ATTN R. CRAWFORD

COMMANDER/DIRECTOR
ATMOSPHERIC SCIENCES LABORATORY
U.S. ARMY ELECTRONICS COMMAND
WHITE SANDS MISSILE RANGE, NM 88002
    01CY ATTN DELAS-EO F. NILES

DIRECTOR
BMD ADVANCED TECH CTR
HUNTSVILLE OFFICE
P. O. BOX 1500
HUNTSVILLE, AL 35807
    01CY ATTN ATC-T MELVIN T. CAPPS
    01CY ATTN ATC-O W. DAVIES
    01CY ATTN ATC-R DON RUSS

PROGRAM MANAGER
BMD PROGRAM OFFICE
5001 EISENHOWER AVENUE
ALEXANDRIA, VA 22333
    01CY ATTN DACS-BMT J. SHEA

CHIEF C-E SERVICES DIVISION
U.S. ARMY COMMUNICATIONS CMD
PENTAGON RM 1B269
WASHINGTON, D.C. 20310
    01CY ATTN C-E-SERVICES DIVISION

COMMANDER
FRADCOM TECHNICAL SUPPORT ACTIVITY
DEPARTMENT OF THE ARMY
FORT MONMOUTH, N.J. 07703
    01CY ATTN DRSEL-NL-RD H. BENNET
    01CY ATTN DRSEL-PL-ENV H. BOMKE
    01CY ATTN J. E. QUIGLEY

COMMANDER
HARRY DIAMOND LABORATORIES
DEPARTMENT OF THE ARMY
2800 POWDER MILL ROAD
ADELPHI, MD 20783
        (CNWDI-INNER ENVELOPE: ATTN: DELHD-RBH)
    01CY ATTN DELHD-TI M. WEINER
    01CY ATTN DELHD-RB R. WILLIAMS
    01CY ATTN DELHD-NP F. WIMENITZ
    01CY ATTN DELHD-NP C. MOAZED

COMMANDER
U.S. ARMY COMM-ELEC ENGRG INSTAL AGY
FT. HUACHUCA, AZ 85613

    01CY ATTN CCC-EMEO GEORGE LANE

COMMANDER
U.S. ARMY FOREIGN SCIENCE & TECH CTR
220 7TH STREET, NE
CHARLOTTESVILLE, VA 22901
    01CY ATTN DRXST-SD
    01CY ATTN R. JONES

COMMANDER
U.S. ARMY MATERIEL DEV & READINESS CMD
5001 EISENHOWER AVENUE
ALEXANDRIA, VA 22333
    01CY ATTN DRCLDC J. A. BENDER

COMMANDER
U.S. ARMY NUCLEAR AND CHEMICAL AGENCY
7500 BACKLICK ROAD
BLDG 2073
SPRINGFIELD, VA 22150
    01CY ATTN LIBRARY

DIRECTOR
U.S. ARMY BALLISTIC RESEARCH LABS
ABERDEEN PROVING GROUND, MD 21005
    01CY ATTN TECH LIB EDWARD BAICY

COMMANDER
U.S. ARMY SATCOM AGENCY
FT. MONMOUTH, NJ 07703
    01CY ATTN DOCUMENT CONTROL

COMMANDER
U.S. ARMY MISSILE INTELLIGENCE AGENCY
REDSTONE ARSENAL, AL 35809
    01CY ATTN JIM GAMBLE

DIRECTOR
U.S. ARMY TRADOC SYSTEMS ANALYSIS ACTIVITY
WHITE SANDS MISSILE RANGE, NM 88002
    01CY ATTN ATAA-SA
    01CY ATTN TCC/F. PAYAN JR.
    01CY ATTN ATAA-TAC LTC J. HESSE

COMMANDER
NAVAL ELECTRONIC SYSTEMS COMMAND
WASHINGTON, D.C. 20360
    01CY ATTN NAVALEX 034 T. HUGHES
    01CY ATTN PME 117
    01CY ATTN PME 117-T
    01CY ATTN CODE 5011

COMMANDING OFFICER
NAVAL INTELLIGENCE SUPPORT CTR
4301 SUITLAND ROAD, BLDG. 5
WASHINGTON, D.C. 20390
    01CY ATTN MR. DUBBIN STIC 12
    01CY ATTN NISC-50
    01CY ATTN CODE 5404 J. GALET

COMMANDER
NAVAL OCEAN SYSTEMS CENTER
SAN DIEGO, CA 92152
    03CY ATTN CODE 532 W MOLER
    01CY ATTN CODE 0230 C. BAGGETT
    01CY ATTN CODE 81 R. EASTMAN

DIRECTOR
NAVAL RESEARCH LABORATORY
WASHINGTON, D.C. 20375
    01CY ATTN CODE 4700 T. P. COFFEY (25 CYS IF UN, 1 CY IF CLASS)
    01CY ATTN CODE 4701 JACK D. BROWN
    01CY ATTN CODE 4780 BRANCH HEAD (150 CYS IF UN, 1 CY IF CLASS)
    01CY ATTN CODE 7500 HQ COMM DIR BRUCE WALD
    01CY ATTN CODE 7550 J. DAVIS
    01CY ATTN CODE 7580
    01CY ATTN CODE 7551
    01CY ATTN CODE 7555
    01CY ATTN CODE 4730 E. MCLEAN
    01CY ATTN CODE 4127 C. JOHNSON

COMMANDER
NAVAL SEA SYSTEMS COMMAND
WASHINGTON, D.C. 20362
    01CY ATTN CAPT R. PITKIN

COMMANDER
NAVAL SPACE SURVEILLANCE SYSTEM
DAHLGREN, VA 22448
    01CY ATTN CAPT J. H. BURTON

OFFICER-IN-CHARGE
NAVAL SURFACE WEAPONS CENTER
WHITE OAK, SILVER SPRING, MD 20910
    01CY ATTN CODE F31

DIRECTOR
STRATEGIC SYSTEMS PROJECT OFFICE
DEPARTMENT OF THE NAVY
WASHINGTON, D.C. 20376
    01CY ATTN NSP-2141
    01CY ATTN NSSP-2722 FRED WIMBERLY

NAVAL SPACE SYSTEM ACTIVITY
P. O. BOX 92960
WORLDWAY POSTAL CENTER
LOS ANGELES, CALIF. 90009
    01CY ATTN A. B. HAZZARD

COMMANDER
NAVAL SURFACE WEAPONS CENTER
DAHLGREN LABORATORY
DAHLGREN, VA 22448
    01CY ATTN CODE DF-14 R. BUTLER

COMMANDING OFFICER
NAVY SPACE SYSTEMS ACTIVITY
P.O. BOX 92960
WORLDWAY POSTAL CENTER
LOS ANGELES, CA. 90009
    01CY ATTN CODE 52

OFFICE OF NAVAL RESEARCH
ARLINGTON, VA 22217
    01CY ATTN CODE 465
    01CY ATTN CODE 461
    01CY ATTN CODE 402
    01CY ATTN CODE 420
    01CY ATTN CODE 421

COMMANDER
AEROSPACE DEFENSE COMMAND/DC
DEPARTMENT OF THE AIR FORCE
ENT AFB, CO 80912
    01CY ATTN DC MR. LONG

COMMANDER
AEROSPACE DEFENSE COMMAND/XPD
DEPARTMENT OF THE AIR FORCE
ENT AFB, CO 80912
    01CY ATTN XPDQQ
    01CY ATTN XP

AIR FORCE GEOPHYSICS LABORATORY
HANSCOM AFB, MA 01731
    01CY ATTN OPR HAROLD GARDNER
    01CY ATTN OPR-1 JAMES C. ULWICK
    01CY ATTN LKB KENNETH S. W. CHAMPION
    01CY ATTN OPR ALVA T. STAIR
    01CY ATTN PHP JULES AARONS
    01CY ATTN PHD JURGEN BUCHAU
    01CY ATTN PHD JOHN P. MULLEN

AF WEAPONS LABORATORY
KIRTLAND AFB, NM 87117
    01CY ATTN SUL
    01CY ATTN CA ARTHUR H. GUENTHER
    01CY ATTN DYC CAPT J. BARRY
    01CY ATTN DYC JOHN M. KAMM
    01CY ATTN DYT CAPT MARK A. FRY
    01CY ATTN DES MAJ GARY GANONG
    01CY ATTN DYC J. JANNI

AFTAC
PATRICK AFB, FL 32925
    01CY ATTN TF/MAJ WILEY
    01CY ATTN TN

AIR FORCE AVIONICS LABORATORY
WRIGHT-PATTERSON AFB, OH 45433
    01CY ATTN AAD WADE HUNT
    01CY ATTN AAD ALLEN JOHNSON

DEPUTY CHIEF OF STAFF
RESEARCH, DEVELOPMENT, & ACQ
DEPARTMENT OF THE AIR FORCE
WASHINGTON, D.C. 20330
    01CY ATTN AFRDQ

HEADQUARTERS
ELECTRONIC SYSTEMS DIVISION/XR
DEPARTMENT OF THE AIR FORCE
HANSCOM AFB, MA 01731
    01CY ATTN XR J. DEAS

HEADQUARTERS
ELECTRONIC SYSTEMS DIVISION/YSEA
DEPARTMENT OF THE AIR FORCE
HANSCOM AFB, MA 01731
    01CY ATTN YSEA

HEADQUARTERS
ELECTRONIC SYSTEMS DIVISION/DC
DEPARTMENT OF THE AIR FORCE
HANSCOM AFB, MA 01731
    01CY ATTN DCKC MAJ J.C. CLARK

COMMANDER
FOREIGN TECHNOLOGY DIVISION, AFSC
WRIGHT-PATTERSON AFB, OH 45433
    01CY ATTN NICD LIBRARY
    01CY ATTN ETDP B. BALLARD

COMMANDER
ROME AIR DEVELOPMENT CENTER, AFSC
GRIFFISS AFB, NY 13441
    01CY ATTN DOC LIBRARY/TSLD
    01CY ATTN OCSE V. COYNE

SAMSO/SZ
POST OFFICE BOX 92960
WORLDWAY POSTAL CENTER
LOS ANGELES, CA 90009
(SPACE DEFENSE SYSTEMS)
    01CY ATTN SZJ

STRATEGIC AIR COMMAND/XPFS
OFFUTT AFB, NB 68113
    01CY ATTN XPFS MAJ B. STEPHAN
    01CY ATTN ADWATE MAJ BRUCE BAUER
    01CY ATTN NRT
    01CY ATTN DOK CHIEF SCIENTIST

SAMSO/SK
P. O. BOX 92960
WORLDWAY POSTAL CENTER
LOS ANGELES, CA 90009
    01CY ATTN SKA (SPACE COMM SYSTEMS) M. CLAVIN

SAMSO/MN
NORTON AFB, CA 92409
(MINUTEMAN)
    01CY ATTN MNNL LTC KENNEDY

COMMANDER
ROME AIR DEVELOPMENT CENTER, AFSC
HANSCOM AFB, MA 01731
    01CY ATTN EEP A. LORENTZEN

DEPARTMENT OF ENERGY
ALBUQUERQUE OPERATIONS OFFICE
P. O. BOX 5400
ALBUQUERQUE, NM 87115
    01CY ATTN DOC CON FOR D. SHERWOOD

DEPARTMENT OF ENERGY
LIBRARY ROOM G-042
WASHINGTON, D.C. 20545
    01CY ATTN DOC CON FOR A. LABOWITZ

EG&G, INC.
LOS ALAMOS DIVISION
P. O. BOX 809
LOS ALAMOS, NM 85544
    01CY ATTN DOC CON FOR J. BREEDLOVE

UNIVERSITY OF CALIFORNIA
LAWRENCE LIVERMORE LABORATORY
P. O. BOX 808
LIVERMORE, CA 94550
    01CY ATTN DOC CON FOR TECH INFO DEPT
    01CY ATTN DOC CON FOR L-389 R. OTT
    01CY ATTN DOC CON FOR L-31 R. HAGER
    01CY ATTN DOC CON FOR L-46 F. SEWARD

LOS ALAMOS SCIENTIFIC LABORATORY
P. O. BOX 1663
LOS ALAMOS, NM 87545
    01CY ATTN DOC CON FOR J. WOLCOTT
    01CY ATTN DOC CON FOR R. F. TASCHEK
    01CY ATTN DOC CON FOR E. JONES
    01CY ATTN DOC CON FOR J. MALIK
    01CY ATTN DOC CON FOR R. JEFFRIES
    01CY ATTN DOC CON FOR J. ZINN
    01CY ATTN DOC CON FOR P. KEATON
    01CY ATTN DOC CON FOR D. WESTERVELT

SANDIA LABORATORIES
P. O. BOX 5800
ALBUQUERQUE, NM 87115
    01CY ATTN DOC CON FOR J. MARTIN
    01CY ATTN DOC CON FOR W. BROWN
    01CY ATTN DOC CON FOR A. THORNBROUGH
    01CY ATTN DOC CON FOR T. WRIGHT
    01CY ATTN DOC CON FOR D. DAHLGREN
    01CY ATTN DOC CON FOR 3141
    01CY ATTN DOC CON FOR SPACE PROJECT DIV

SANDIA LABORATORIES
LIVERMORE LABORATORY
P. O. BOX 969
LIVERMORE, CA 94550
    01CY ATTN DOC CON FOR B. MURPHEY
    01CY ATTN DOC CON FOR T. COOK

OFFICE OF MILITARY APPLICATION
DEPARTMENT OF ENERGY
WASHINGTON, D.C. 20545
    01CY ATTN DOC CON FOR D. GALE

OTHER GOVERNMENT

CENTRAL INTELLIGENCE AGENCY
ATTN RD/SI, RM 5G48, HQ BLDG
WASHINGTON, D.C. 20505
    01CY ATTN OSI/PSID RM 5F 19

DEPARTMENT OF COMMERCE
NATIONAL BUREAU OF STANDARDS
WASHINGTON, D.C. 20234
    (ALL CORRES: ATTN SEC OFFICER FOR)
    01CY ATTN R. MOORE

INSTITUTE FOR TELECOM SCIENCES
NATIONAL TELECOMMUNICATIONS & INFO ADMIN
BOULDER, CO 80303
    01CY ATTN A. JEAN (UNCLASS ONLY)
    01CY ATTN W. UTLAUT
    01CY ATTN D. CROMBIE
    01CY ATTN L. BERRY

NATIONAL OCEANIC & ATMOSPHERIC ADMIN
ENVIRONMENTAL RESEARCH LABORATORIES
DEPARTMENT OF COMMERCE
BOULDER, CO 80302
    01CY ATTN R. GRUBB
    01CY ATTN AERONOMY LAB G. REID

DEPARTMENT OF DEFENSE CONTRACTORS

AEROSPACE CORPORATION
P. O. BOX 92957
LOS ANGELES, CA 90009
    01CY ATTN I. GARFUNKEL
    01CY ATTN T. SALMI
    01CY ATTN V. JOSEPHSON
    01CY ATTN S. BOWER
    01CY ATTN N. STOCKWELL
    01CY ATTN D. OLSEN

    01CY ATTN SMFA FOR PWW

ANALYTICAL SYSTEMS ENGINEERING CORP
5 OLD CONCORD ROAD
BURLINGTON, MA 01803
    01CY ATTN RADIO SCIENCES

BERKELEY RESEARCH ASSOCIATES, INC.
P. O. BOX 983
BERKELEY, CA 94701
    01CY ATTN J. WORKMAN

BOEING COMPANY, THE
P. O. BOX 3707
SEATTLE, WA 98124
    01CY ATTN G. KEISTER
    01CY ATTN D. MURRAY
    01CY ATTN G. HALL
    01CY ATTN J. KENNEY

CALIFORNIA AT SAN DIEGO, UNIV OF

P.O. Box 6049

San Diego, CA 92106

BROWN ENGINEERING COMPANY, INC.
CUMMINGS RESEARCH PARK
HUNTSVILLE, AL 35807
    01CY ATTN ROMEO A. DELIBERIS

CHARLES STARK DRAPER LABORATORY, INC.
555 TECHNOLOGY SQUARE
CAMBRIDGE, MA 02139
    01CY ATTN D. B. COX
    01CY ATTN J. P. GILMORE

COMPUTER SCIENCES CORPORATION
6565 ARLINGTON BLVD
FALLS CHURCH, VA 22046
    01CY ATTN H. BLANK
    01CY ATTN JOHN SPOOR
    01CY ATTN C. NAIL

COMSAT LABORATORIES
LINTHICUM ROAD
CLARKSBURG, MD 20734
    01CY ATTN G. HYDE

CORNELL UNIVERSITY
DEPARTMENT OF ELECTRICAL ENGINEERING
ITHACA, NY 14850
    01CY ATTN D. T. FARLEY JR

ELECTROSPACE SYSTEMS, INC.
BOX 1359
RICHARDSON, TX 75080
    01CY ATTN H. LOGSTON
    01CY ATTN SECURITY (PAUL PHILLIPS)

ESL INC.
495 JAVA DRIVE
SUNNYVALE, CA 94086
    01CY ATTN J. ROBERTS
    01CY ATTN JAMES MARSHALL
    01CY ATTN C. W. PRETTIE

FORD AEROSPACE & COMMUNICATIONS CORP
3939 FABIAN WAY
PALO ALTO, CA 94303
    01CY ATTN J. T. MATTINGLEY

GENERAL ELECTRIC COMPANY
SPACE DIVISION
VALLEY FORGE SPACE CENTER
GODDARD BLVD KING OF PRUSSIA
P. O. BOX 8555
PHILADELPHIA, PA 19101
    01CY ATTN M. H. BORTNER SPACE SCI LAB

GENERAL ELECTRIC COMPANY
P. O. BOX 1122
SYRACUSE, NY 13201
    01CY ATTN F. REIBERT

GENERAL ELECTRIC COMPANY
TEMPO-CENTER FOR ADVANCED STUDIES
816 STATE STREET (P.O. DRAWER QQ)
SANTA BARBARA, CA 93102
    01CY ATTN DASIAC
    01CY ATTN DON CHANDLER
    01CY ATTN TOM BARRETT
    01CY ATTN TIM STEPHANS
    01CY ATTN WARREN S. KNAPP
    01CY ATTN WILLIAM MCNAMARA
    01CY ATTN B. GAMBILL
    01CY ATTN MACK STANTON

GENERAL ELECTRIC TECH SERVICES CO., INC.
HMES
COURT STREET
SYRACUSE, NY 13201
    01CY ATTN G. MILLMAN

GENERAL RESEARCH CORPORATION
SANTA BARBARA DIVISION
P. O. BOX 6770
SANTA BARBARA, CA 93111
    01CY ATTN JOHN ISE JR
    01CY ATTN JOEL GARBARINO

GEOPHYSICAL INSTITUTE
UNIVERSITY OF ALASKA
FAIRBANKS, AK 99701
      (ALL CLASS ATTN: SECURITY OFFICER)
    01CY ATTN T. N. DAVIS (UNCL ONLY)
    01CY ATTN NEAL BROWN (UNCL ONLY)
    01CY ATTN TECHNICAL LIBRARY

GTE SYLVANIA, INC.
ELECTRONICS SYSTEMS GRP-EASTERN DIV
77 A STREET
NEEDHAM, MA 02194
    01CY ATTN MARSHAL CROSS

ILLINOIS, UNIVERSITY OF
DEPARTMENT OF ELECTRICAL ENGINEERING
URBANA, IL 61803
    01CY ATTN K. YEH

ILLINOIS, UNIVERSITY OF
107 COBLE HALL
801 S. WRIGHT STREET
URBANA, IL 60680
      (ALL CORRES ATTN SECURITY SUPERVISOR FOR)
    01CY ATTN K. YEH

INSTITUTE FOR DEFENSE ANALYSES
400 ARMY-NAVY DRIVE
ARLINGTON, VA 22202
    01CY ATTN J. M. AEIN
    01CY ATTN ERNEST BAUER
    01CY ATTN HANS WOLFHARD
    01CY ATTN JOEL BENGSTON

HSS, INC.
2 ALFRED CIRCLE
BEDFORD, MA 01730
    01CY ATTN DONALD HANSEN

INTL TEL & TELEGRAPH CORPORATION
500 WASHINGTON AVENUE
NUTLEY, NJ 07110
    01CY ATTN TECHNICAL LIBRARY

JAYCOR
1401 CAMINO DEL MAR
DEL MAR, CA 92014
    01CY ATTN S. R. GOLDMAN

JOHNS HOPKINS UNIVERSITY
APPLIED PHYSICS LABORATORY
JOHNS HOPKINS ROAD
LAUREL, MD 20810
    01CY ATTN DOCUMENT LIBRARIAN
    01CY ATTN THOMAS POTEMRA
    01CY ATTN JOHN DASSOULAS

LOCKHEED MISSILES & SPACE CO INC
P. O. BOX 504
SUNNYVALE, CA 94088
    01CY ATTN DEPT 60-12
    01CY ATTN D. R. CHURCHILL

LOCKHEED MISSILES AND SPACE CO INC
3251 HANOVER STREET
PALO ALTO, CA 94304
    01CY ATTN MARTIN WALT DEPT 52-10
    01CY ATTN RICHARD G. JOHNSON DEPT 52-12
    01CY ATTN W. L. IMHOF DEPT 52-12

KAMAN SCIENCES CORP
P. O. BOX 7463
COLORADO SPRINGS, CO 80933
    01CY ATTN T. MEAGHER

LINKABIT CORP
10453 ROSELLE
SAN DIEGO, CA 92121
    01CY ATTN IRWIN JACOBS

M.I.T. LINCOLN LABORATORY
P. O. BOX 73
LEXINGTON, MA 02173
    01CY ATTN DAVID M. TOWLE
    01CY ATTN P. WALDRON
    01CY ATTN L. LOUGHLIN
    01CY ATTN D. CLARK

MARTIN MARIETTA CORP
ORLANDO DIVISION
P. O. BOX 5837
ORLANDO, FL 32805
    01CY ATTN R. HEFFNER

MCDONNELL DOUGLAS CORPORATION
5301 BOLSA AVENUE
HUNTINGTON BEACH, CA 92647
    01CY ATTN N. HARRIS
    01CY ATTN J. MOULE
    01CY ATTN GEORGE MROZ
    01CY ATTN W. OLSON
    01CY ATTN R. W. HALPRIN
    01CY ATTN TECHNICAL LIBRARY SERVICES

MISSION RESEARCH CORPORATION
735 STATE STREET
SANTA BARBARA, CA 93101
    01CY ATTN P. FISCHER
    01CY ATTN W. F. CREVIER
    01CY ATTN STEVEN L. GUTSCHE
    01CY ATTN D. SAPPENFIELD
    01CY ATTN R. BOGUSCH
    01CY ATTN R. HENDRICK
    01CY ATTN RALPH KILB
    01CY ATTN DAVE SOWLE
    01CY ATTN F. FAJEN
    01CY ATTN M. SCHEIBE
    01CY ATTN CONRAD L. LONGMIRE
    01CY ATTN WARREN A. SCHLUETER

MITRE CORPORATION, THE
P. O. BOX 208
BEDFORD, MA 01730
    01CY ATTN JOHN MORGANSTERN
    01CY ATTN G. HARDING
    01CY ATTN C. E. CALLAHAN

MITRE CORP
WESTGATE RESEARCH PARK
1820 DOLLY MADISON BLVD
MCLEAN, VA 22101
    01CY ATTN W. HALL
    01CY ATTN W. FOSTER

PACIFIC-SIERRA RESEARCH CORP
1456 CLOVERFIELD BLVD.
SANTA MONICA, CA 90404
    01CY ATTN E. C. FIELD JR

PENNSYLVANIA STATE UNIVERSITY
IONOSPHERE RESEARCH LAB
318 ELECTRICAL ENGINEERING EAST
UNIVERSITY PARK, PA 16802
    (NO CLASSIFIED TO THIS ADDRESS)
    01CY ATTN IONOSPHERIC RESEARCH LAB

PHOTOMETRICS, INC.
442 MARRETT ROAD
LEXINGTON, MA 02173
    01CY ATTN IRVING L. KOFSKY

PHYSICAL DYNAMICS INC.
P. O. BOX 3027
BELLEVUE, WA 98009
    01CY ATTN E. J. FREMOUW

PHYSICAL DYNAMICS INC.
P. O. BOX 10367
OAKLAND, CA. 94610
    ATTN: A. THOMSON

R & D ASSOCIATES
P. O. BOX 9695
MARINA DEL REY, CA 90291
    01CY ATTN FORREST GILMORE
    01CY ATTN BRYAN GABBARD
    01CY ATTN WILLIAM B. WRIGHT JR
    01CY ATTN ROBERT F. LELEVIER
    01CY ATTN WILLIAM J. KARZAS
    01CY ATTN H. ORY
    01CY ATTN C. MACDONALD
    01CY ATTN R. TURCO

RAND CORPORATION, THE
1700 MAIN STREET
SANTA MONICA, CA 90406
    01CY ATTN CULLEN CRAIN
    01CY ATTN ED BEDROZIAN

RIVERSIDE RESEARCH INSTITUTE
80 WEST END AVENUE
NEW YORK, NY 10023
    01CY ATTN VINCE TRAPANI

SCIENCE APPLICATIONS, INC.
P. O. BOX 2351
LA JOLLA, CA 92038
    01CY ATTN LEWIS M. LINSON
    01CY ATTN DANIEL A. HAMLIN
    01CY ATTN D. SACHS
    01CY ATTN E. A. STRAKER
    01CY ATTN CURTIS A. SMITH
    01CY ATTN JACK MCDOUGALL

RAYTHEON CO.
528 BOSTON POST ROAD
SUDBURY, MA 01776
    01CY ATTN BARBARA ADAMS

SCIENCE APPLICATIONS, INCORPORATED
1710 Goodridge Dr.
McLean, VA 22102
  Attn: J. Cockayne

Lockheed Missile & Space Co., Inc.
Huntsville Research & Engr. Ctr.
4800 Bradford Drive
Huntsville, Alabama 35807
Attn: Dale H. Davis

SRI INTERNATIONAL
333 RAVENSWOOD AVENUE
MENLO PARK, CA 94025
    01CY ATTN DONALD NEILSON
    01CY ATTN ALAN BURNS
    01CY ATTN G. SMITH
    01CY ATTN L. L. COBB
    01CY ATTN DAVID A. JOHNSON
    01CY ATTN WALTER G. CHESNUT
    01CY ATTN CHARLES L. RINO
    01CY ATTN WALTER JAYE
    01CY ATTN M. BARON
    01CY ATTN RAY L. LEADABRAND
    01CY ATTN G. CARPENTER
    01CY ATTN G. PRICE
    01CY ATTN J. PETERSON
    01CY ATTN R. HAKE, JR.
    01CY ATTN V. GONZALES
    01CY ATTN D. MCDANIEL

TECHNOLOGY INTERNATIONAL CORP
75 WIGGINS AVENUE
BEDFORD, MA 01730
    01CY ATTN W. P. BOQUIST

TRW DEFENSE & SPACE SYS GROUP
ONE SPACE PARK
REDONDO BEACH, CA 90278
    01CY ATTN R. K. PLEBUCH
    01CY ATTN S. ALTSCHULER
    01CY ATTN D. DEE

VISIDYNE, INC.
19 THIRD AVENUE
NORTH WEST INDUSTRIAL PARK
BURLINGTON, MA 01803
    01CY ATTN CHARLES HUMPHREY
    01CY ATTN J. W. CARPENTER